

^2H NMR and X-ray diffraction studies of methyl rotation in crystals of *ortho*-methyldibenzocycloalkanones

Deniz Cizmeciyan^a, Heather Yonutas^a, Steven D. Karlen^b, Miguel A. Garcia-Garibay^{b,*}

^aMount St. Mary's College, 12001 Chalon Road, Los Angeles, CA 90049, USA

^bDepartment of Chemistry and Biochemistry, University of California, 607, Charles E. Young Drive East, Los Angeles, CA 90095-1569, USA

Received 16 November 2004; received in revised form 22 February 2005

Available online 31 March 2005

Abstract

We have used ^2H NMR lineshape analyses and single crystal X-ray diffraction (XRD) to investigate the effects of molecular structure and crystalline environment on the rotational dynamics of methyl groups in four aromatic cycloalkanones. These include two methyl-substituted anthrones, one anthraquinone and one dibenzosuberone, which are known to undergo excited state H-atom tunneling from the *ortho*-methyl group to the carbonyl oxygen. With experiments conducted between 100 and 300 K, samples 1,4-dimethylantrone (DMAT) and 1,4-dimethylantraquinone (DMAQ) were shown to enter the intermediate exchange regime ($k_{\text{rot}} \sim < 10^7 \text{ s}^{-1}$) at ca. 120 K while samples of 1,4,10,10-tetramethylantrone (TMAT) and 1,4-dimethyldibenzosuberone (DMDBS) remained in the fast exchange regime even at ca. 100 K. Single crystal XRD analyses suggest that high intramolecular hindrance is avoided by molecular distortions, and that intermolecular contacts play an important role.

© 2005 Elsevier Inc. All rights reserved.

Keywords: Methyl rotation; *Ortho*-methyl ketones; ^2H NMR; X-ray diffraction

1. Introduction

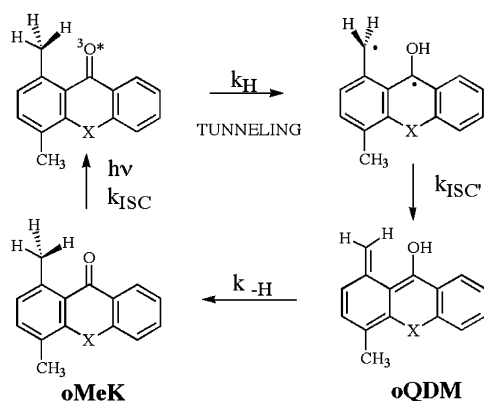
In the last few years, we have investigated the photo-induced hydrogen atom transfer reaction of several *ortho*-methyl arylketones (*o*MeK) to *ortho*-quinodimethanes (*o*QDM) as a simple model to document structural and kinetic aspects of quantum mechanical tunneling [1]. As shown in Scheme 1, the reaction occurs by transfer of a hydrogen atom from the methyl group to the singly occupied n-orbital of the $^3n, \pi^*$ excited carbonyl and it occurs in a reversible manner. Although we have investigated several aromatic ketones [2], the structure of 1,4-dimethylantrone (DMAT) (Scheme 1, X = CH₂, and in Scheme 2), is particularly interesting because the tunneling reaction is remarkably efficient. In

fact, the rate of H-transfer in DMAT is too fast to be measured within the time resolution of our cryogenic setup ($k_{\text{H}} \geq 10^7 \text{ s}^{-1}$) even at 4 K, suggesting that the methyl group and carbonyl oxygen exist at a distance and orientation that make H-transfer particularly efficient. To carry out detailed kinetic measurements we had to take advantage of a large primary kinetic isotope effect (ca. $k_{\text{H}}/k_{\text{D}} > 10^3$) with samples of DMAT-*d*₈ (Scheme 2).

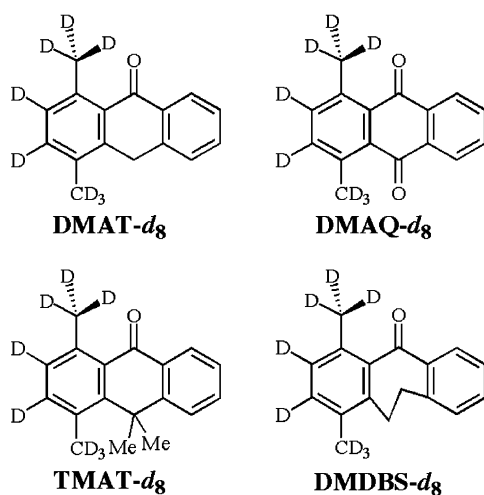
Although fast methyl rotation under the condition of triplet state quantum mechanical tunneling reaction at 4 K is not expected, it was of interest to see whether the steric interaction between the methyl and carbonyl groups of DMAT may result in unusually high rotational barriers. In addition, it was recently shown by Casadesus et al. [3] that changes in molecular geometry upon electronic excitation are relatively small, suggesting that similar trends may be expected in both ground and excited state rotational profiles. In this paper, we would like to report measurements of methyl

*Corresponding authors. Fax: +1 310 954 4379 (DC); +1 310 825 0767 (MGG).

E-mail addresses: dcizmeciyan@msmc.la.edu, mgg@chem.ucla.edu (M.A. Garcia-Garibay).



Scheme 1.



Scheme 2.

rotation in DMAT and three other ketones by quadrupolar echo ^2H NMR and their analysis in terms of structures determined by single crystal X-ray diffraction (XRD) studies. The method and its application have been reviewed [4]. It relies on the analysis of spectral changes caused by dynamic averaging of the orientation-dependent interaction between the ^2H nuclear electric quadrupolar moment and the electric field gradient (EFG) at the nuclear position. Variations in line shape caused by site exchange among magnetically non-equivalent sites are generally accounted for by a three-fold jump model which is highly sensitive to exchange occurring between 10^7 and 10^4 Hz [5,6]. Arrhenius' analysis of rate measurements carried out as a function of temperature provide activation energies, which are expected to reflect local steric crowding or any other hindering potential. ^2H spectroscopy has been successfully used for understanding dynamics in biological systems [7], polymers [8], liquid crystals [9], clathrates [10], and recently, in molecular compasses and gyroscopes [11].

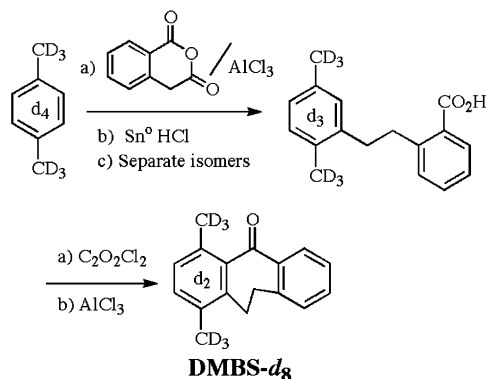
In addition to 1,4-dimethylantrone- d_8 (DMAT- d_8) we analyzed three related compounds with relatively small structural variations with hopes that they should affect the local environment of their methyl groups and their rotation barriers (Scheme 2). These are 1,4-dimethylantraquinone- d_8 (DMAQ- d_8), 1,4,10,10-tetramethylantrone- d_8 (TMAT- d_8), and 1,4-dimethyldibenzosuberone- d_8 (DMDBS- d_8). In general, our results revealed that the effect of the *ortho*-carbonyl in these compounds is modest. Although we were able to ascertain that two methyl groups in DMAT- d_8 are dynamically distinguishable, their exchange rates were barely slowed down to the upper limit of the line shape analysis method (ca. 10^6 – 10^7 s $^{-1}$) at ca. 120 K. Samples of DMAQ- d_8 were obtained and analyzed, DMAQ has a C_{2v} symmetric molecular structure which in solution has only one methyl signal. In the crystalline state DMAQ with two methyl groups have clearly distinguishable rotational dynamics. Samples of DMDBS- d_8 were analyzed with the expectation that its seven-membered ring would remove the nearly parallel alignment while increasing the distance of the methyl and carbonyl groups. In fact, methyl group rotation in DMDBS- d_8 occurs within the fast exchange limit with $k_{\text{rot}} > 10^7$ s $^{-1}$ even at 100 K. Finally, the two methyl groups at C10 in TMAT- d_8 were expected to cause severe steric crowding to the methyl group at C4. Remarkably, with a significant distortion in the ketone structure, the rotation of the two aromatic methyl in TMAT- d_8 was significantly faster than that in DMAT- d_8 or DMAQ- d_8 . In search of a qualitative explanation between the different dynamics of these compounds we also carried out a single crystal XRD analyses of all four compounds.

2. Experimental section

All four *ortho*-methyl ketones investigated in this study are known compounds. We reported the synthesis of DMAQ- d_8 and DMAT- d_8 in a previous paper [1a]. Samples of 1,4,10,10-tetramethylantrone (TMAT- d_8) were prepared by base-catalyzed MeI alkylation of DMAT- d_8 as reported by Curtin et al. [12]. DMDBS- d_8 was prepared as illustrated in Scheme 3 from *para*-xylene- d_8 and homophthalic anhydride [13]. The structures of TMAT- d_8 and DMDBS- d_8 were also confirmed by single crystal XRD analyses.

2.1. NMR measurements

^2H NMR measurements of *ortho*-methyl arylketones were carried out at 46.073 MHz on a Bruker Avance instrument. A solenoid single channel probe with a 5 mm insert was used. In all cases pulse widths and phases were carefully adjusted before recording the



Scheme 3.

spectra, which were acquired using the quadrupole echo pulse sequence. The 90° pulse lengths were typically $2.5\ \mu\text{s}$ with echo delays of 30 and $20\ \mu\text{s}$, respectively. Recycle delays were approximately five times the methyl groups T_1 's, from 2 to 30 s at 298 and 115 K, respectively. These recycle delays are not long enough to allow for complete relaxation of the aromatic deuterons so that relative intensity comparisons between the two types of signals are not meaningful. Temperature determinations were carried out with a copper–constantan thermocouple carefully positioned near the sample.

2.2. ^2H line shape simulations

Spectra were fit with the program Turbopowder [14]. The input to the program consists of a model with the proper exchange geometries, site populations, and exchange rates. A series of QCC constants were simulated for both the methyl and aromatic deuterons, the optimal QCC values were found to be 160 ± 3 and 179 ± 3 kHz, respectively. The asymmetry parameter (η) was assumed to be 0 in all cases. The QCC and η values agree with those reported in previous studies by Rice et al. [7a] and Copie et al. [7d]. The line broadening used was 3 kHz. The line shape simulations for different types of methyl groups and aromatic deuterons were done individually and the experimental line shape was generated by adding the individual simulations. Exchange rates were obtained by visual comparison of the experimental and simulated spectra.

2.3. Single crystal X-ray diffraction (XRD) determinations

XRD quality crystals of DMDBS and TMAT were readily available by slow solvent evaporation from hexanes. Good quality single crystals of DMAT and DMAQ were significantly more difficult to obtain. The main crystallographic acquisition and refinement

parameter for the three structures are included in Table 1. Detailed crystallographic acquisition, structure solution, and refinement parameters in the form crystallographic information files (CIF) are available upon request.

3. Results

3.1. ^2H NMR of 1,4-dimethylantrone

Deuterium quadrupolar Pake patterns and related simulations at different temperatures are shown in Fig. 1. The line shape of experimental data down to 128 K could be simulated by spectra that assumes a fast exchange three-fold jump model with a rate $>10^7\ \text{s}^{-1}$. Spectra measured between 128 and 111 K revealed clear broadening and an increased intensity for the signals corresponding to the aromatic deuterons, which have a shorter spin-lattice relaxation time at lower temperatures. In addition to the signal corresponding to the static aromatic deuterons, simulations of the lowest temperature spectra required two types of methyl groups. For example, simulations at 115 K required contributions from the static aromatic deuterons, and two methyl groups with exchange rates of 8×10^6 and $10^5\ \text{s}^{-1}$ (Fig. 1)

3.2. ^2H NMR of 1,4-dimethylantraquinone

The Pake patterns of DMAQ- d_8 at different temperatures are shown in Fig. 2 along with simulations obtained using parameters such as those used to simulate the spectra of DMAT- d_8 . Intermediate exchange rates ($\leq 10^7\ \text{s}^{-1}$) in DMAQ- d_8 began to occur at 126 K, suggesting that methyl rotation in this compound may have a slightly higher barrier than that in DMAT- d_8 . Two non-equivalent methyl groups are required to simulate the lower temperature spectra, indicating a lower than expected molecular symmetry. The experimental spectrum is in close agreement with the simulations and shows that both methyl groups rotate in the fast regime at room temperature and intermediate regime at 115 K. The aromatic deuterons are not observed at room temperature due to their slow spin lattice relaxation but can be seen at lower temperatures. The ^{13}C CPMAS spectrum for 1,4-dimethylantraquinone (Fig. 3) clearly shows two distinct methyl groups with different relaxation times of 1.18 and 1.21 s suggesting either a non-symmetric conformation, or two distinct (but symmetric) molecules per asymmetric unit in the crystal. The XRD structure of DMAQ revealed the former to be the case with one non-symmetric molecule per asymmetric unit.

Table 1
Main crystallographic parameters

| | DMAQ ^a | DMAT ^a | DMDBS ^b | TMAT ^b |
|---|--|-----------------------------------|-----------------------------------|-----------------------------------|
| Empirical formula | C ₁₆ H ₁₂ O ₂ | C ₁₆ H ₁₄ O | C ₁₇ H ₁₆ O | C ₁₈ H ₁₈ O |
| Formula weight | 236.26 | 222.27 | 236.30 | 250.32 |
| Crystal system | Monoclinic | Monoclinic | Triclinic | Monoclinic |
| Space group | P2 ₁ /c | P2/c | P-1 | P2 ₁ /a |
| Size (mm ³) | 0.80 × 0.20 × 0.2 | 0.80 × 0.20 × 0.10 | 0.40 × 0.32 × 0.30 | 0.40 × 0.10 × 0.05 |
| Color | Colorless | Colorless | Colorless | Colorless |
| Morphology | Parallelepiped | Parallelepiped | Parallelepiped | Parallelepiped |
| Temperature (K) | 120(2) | 296(2) | 300(2) | 293(2) |
| <i>a</i> (Å) | 6.8018(8) | 15.6495(18) | 8.8383(6) | 12.235(4) |
| <i>b</i> (Å) | 15.3748(17) | 5.0338(6) | 10.0673(7) | 16.900(5) |
| <i>c</i> (Å) | 11.1590(12) | 16.0919(19) | 8.1127(6) | 14.701(4) |
| α (deg) | 90.00 | 90.00 | 75.522(4) | 90.00 |
| β (deg) | 96.818(2) | 110.984 | 94.700(4) | 113.94(2) |
| γ (deg) | 90.00 | 90.00 | 71.871(3) | 90.00 |
| <i>V</i> (Å ³) | 1158.7(2) | 1183.6(2) | 654.15(8) | 2778.1(13) |
| <i>Z</i> | 4 | 4 | 2 | 8 |
| ρ_{calc} (mg/m ³) | 1.354 | 1.247 | 1.20 | 1.197 |
| Total reflections | 10521 | 10073 | 4314 | 1789 |
| Indep. reflect. | 2799 | 2874 | 1203 | 1297 |
| <i>R</i> (Int) | 0.0210 | 0.0284 | 0.066 | 0.053 |
| <i>R</i> ₁ [<i>I</i> > 3 σ (<i>I</i>)] | | | 0.066 | 0.053 |
| <i>R</i> ₁ [<i>I</i> > 2 σ (<i>I</i>)] | 0.0506 | 0.0485 | | |
| <i>WR</i> ₂ (all data) | 0.1594 | 0.1440 | | |

^aData acquired on a Bruker Smart 1000 K diffractometer equipped with a area detector and a Mo X-ray source. Structural refinement was performed through least-square refinement of F^2 .

^bData acquired on a Rigaku Afc5r diffractometer equipped with a point detector and a Cu X-ray source. Structural refinement was performed through least-square refinement on F .

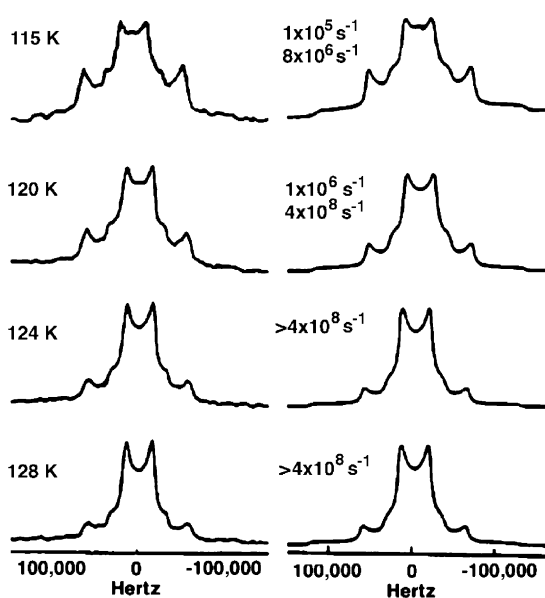


Fig. 1. Left: experimental quadrupolar echo ²H NMR spectra of DMAT-*d*₈ acquired at the temperatures indicated (from top to bottom (K): 115, 120, 124 and 128). Right: simulation of the experimental spectra assuming static aromatic deuterons and the methyl exchange with the rates indicated. No changes in the spectrum were observed at higher temperatures.

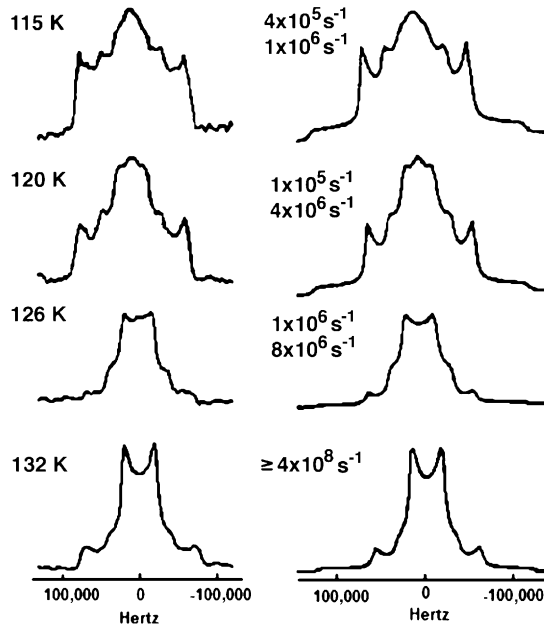


Fig. 2. Left: experimental quadrupolar echo ²H NMR spectra of DMAQ-*d*₈ acquired at the temperatures shown (from bottom to top (K): 132, 126, 120, 115). Right: simulation of the experimental spectra with static aromatic deuterons and the methyl exchange rates indicated.

3.3. ^2H NMR of 1,4-dimethyldibenzosuberone

Quadrupolar echo spectra acquired between 298 and 100 K showed no significant variations indicating that methyl rotation occurs within the fast exchange limit within this temperature range (Fig. 4a).

3.4. ^2H NMR of 1,4,10,10-tetramethylantrone

The incorporation of the two methyl groups at C10 severely crowd the methyl group at C4, as compared to DMAT. This crowding, however, does not slow rotation of the methyl groups as shown by the fact that both methyl groups in TMAT remain in the fast exchange limit down to 120 K (Fig. 4b).

3.5. XRD analysis

Crystals of DMAT were obtained from hexanes as thin plates. The structure was solved in the monoclinic space group $P2_1/c$ with four molecules per unit cell. Molecules of DMAT were found to present a crystallographic disorder where lattice sites corresponding to the CO and CH_2 groups can be occupied by either group with equal probability. A structure representing the two overlapping molecular occupancies is illustrated in Fig. 5. The structure of DMAT has its three rings

coplanar. A slight distortion of the methyl groups can be detected by an angle 176.7° formed between points at the methyl carbons and the center of the phenyl ring. The distance between the *ortho*-methyl and carbonyl oxygen is 2.632 \AA , and the two bonds are essentially coplanar as suggested by a $\text{O}=\text{C}--\text{C}-\text{Me}$ dihedral of only 1.673° .

Single crystals of DMAQ were obtained from hexanes as thin plates. The structure was solved in the monoclinic space group $P2_1/c$ with four molecules per unit cell. Although the molecule possesses a C_2 axis of symmetry and a mirror plane, there are no coincident molecular and crystallographic symmetries making each atom in the structure crystallographically and magnetically non-equivalent (Fig. 6). The distance between the *ortho*-methyl and carbonyl oxygen are 2.686 and 2.688 \AA . The molecule is slightly bent out of planarity as suggested by $\text{O}=\text{C}-\text{C}-\text{Me}$ dihedrals of 2.438° , 1.803° . In addition to the slight bending of the molecule, the two methyl groups are pushed towards the outside of the molecule by the carbonyl as detected by the two methyls forming angles 175.43° and 174.71° with the plane of the phenyl ring.

The crystal structure of DMDBS was solved in the triclinic space group with $P\bar{1}$ only one molecule per asymmetric unit. As shown in Fig. 7, the seven-membered ring in the DMDBS structure adopts a

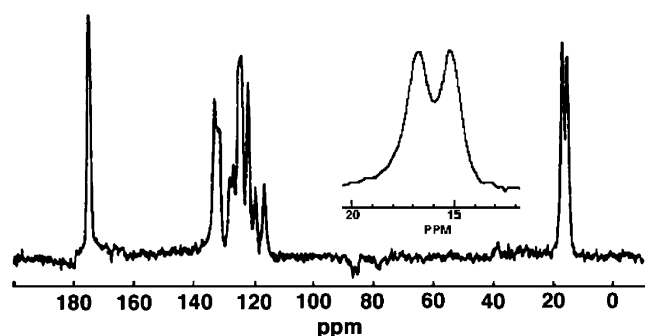


Fig. 3. ^{13}C CPMAS NMR spectrum of DMAQ- d_8 showing two distinct resonances for the aromatic methyl groups at ca. 14 and 16 ppm.

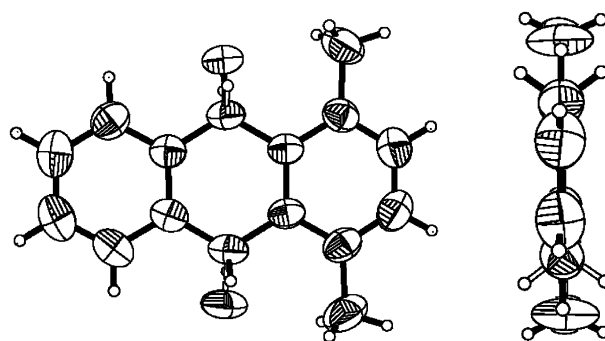


Fig. 5. Front and side views of one of the two positionally disordered molecules of DMAT. The carbonyl and CH_2 groups have 50% occupancies at the central carbons C9 and C10.

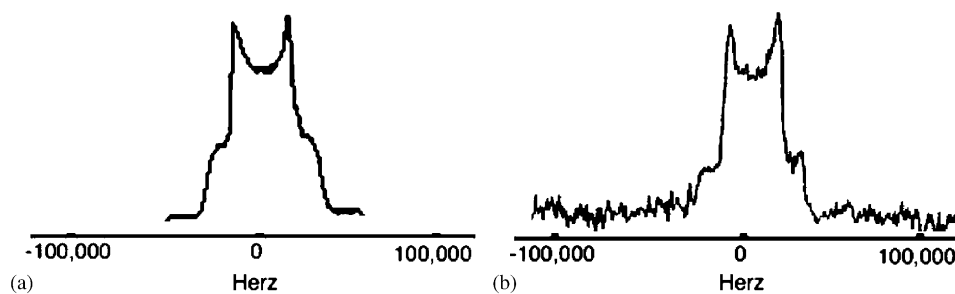


Fig. 4. Quadrupolar echo ^2H NMR spectra of (a) DMDBS- d_8 acquired at 100 K and (b) TMAT- d_8 at 120 K, both showing a pattern characteristic of three-fold methyl jump in the fast exchange limit.

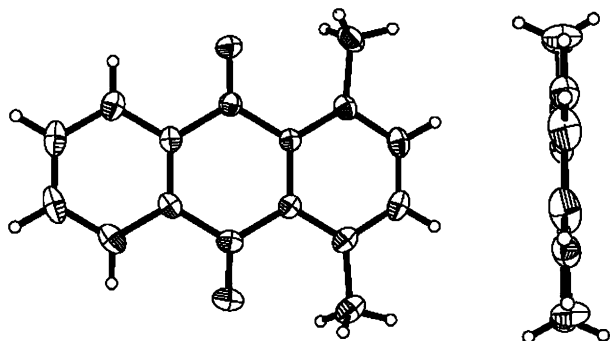


Fig. 6. Front and side views from the XRD structure of DMAQ illustrating some deviation of the C=O and C-CH₃ bond vectors and the planarity of the structure, respectively.

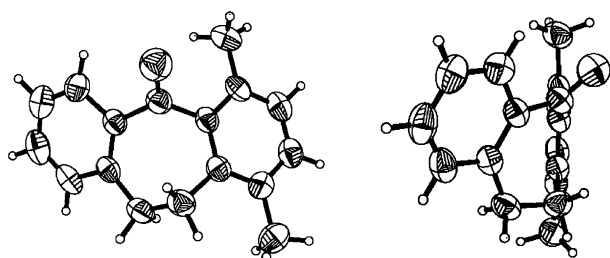


Fig. 7. Front and side views from the XRD structure of DMDBS illustrating the twist-boat conformation of the seven-membered ring and the large deviation of the C=O group from conjugation with the aryl groups.

twist-boat conformation [15] which tilts the two benzene rings in the same direction. The dihedral angles between the planes of each phenyl group and the carbonyl oxygen are 51° and -67°, respectively. The environment around the two methyl groups is not highly crowded. A torsion angle of 56° between the C=O and C-Me bonds extends the distance between the methyl carbon and the carbonyl oxygen from 2.632 Å in DMAT to 3.139 Å in DMDBS. The methyl group at C4 is at distance of 3.021 Å from the closest CH₂ group. It should be noted that these distances are still less than sum of the van der Waals radii for carbon and oxygen (3.2 Å) and carbon-to-carbon (3.7 Å), suggesting a significant crowding for the hydrogen atoms at C11 and C15, which occupy their intervening space.

The structure of TMAT was solved in the monoclinic space group P2₁/a with two molecules per asymmetric unit and eight molecules per unit cell. The molecular structures of TMAT are characterized by having their three rings relatively coplanar but with obvious distortions caused by the steric crowding between the aromatic methyl group at C4 and the two quaternary methyls at C10, Fig. 8. Although the two molecules in the structure are generally similar, they differ in detail. The C-O distance between the methyl at C1 and the carbonyl oxygen varies from 2.659 for molecule 1 to

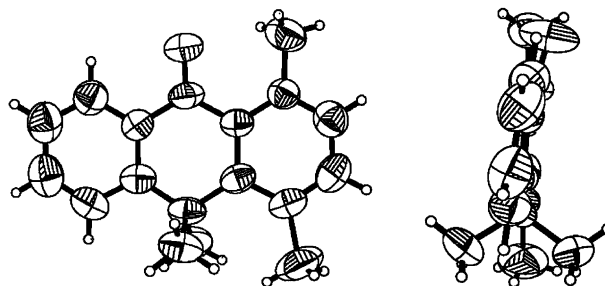


Fig. 8. Front and side views of molecule 1 in crystals of TMAT illustrating the relatively large distortion of the aromatic methyl at C4 and the moderate twisting of the otherwise coplanar rings. The structure of molecule 2 is very similar.

2.702 for molecule 2. The most obvious distortion is given by the non-linearity of the two methyl groups at C1 and C4. The angles formed between C1, the center of the benzene ring, and C4 are 172.2° for molecule 1 and 172.4° for molecule 2.

In search of a possible correlation between the onset of intermediate exchange and the local environment of the aromatic methyl groups we analyzed the packing structures of all four ketones. With each aromatic group as a point of reference, we measured all the non-bonded distances between heavy atoms [C---C and C---O] within 4 Å, and all the H---H and H---O distances within 3.5 Å. With these limits, our analysis considers only atoms that are significantly (0.2–0.4 Å) closer than the sum of the van der Waals distances between the -CH₃ group (2.7 Å) and the C (1.7 Å), O (1.5 Å) and H (1.2 Å) atoms in neighboring molecules. When the results were analyzed, we noticed a clear difference in Me---O=C distances in DMAQ and DMAT as compared to those in DMDBS and TMAT. There were nine contacts within 4 Å, seven of which were within 3.7 Å in the former two, as compared to the three contacts within 4 Å, of which none were within 3.7 Å on the latter structures. We also determined H---H and H---O distances within 3.5 Å of the aromatic methyl protons. Although there is significant uncertainty in hydrogen positions, some qualitative conclusions in full agreement with the heavy atom distances may be drawn from this analysis. Notably, non-bonded contacts in DMAQ and DMAT are significantly shorter as compared to those in DMDBS and TMAT. A closer look suggested that the short C---O distances reveal weak C-H...O hydrogen bonds, as described by the C---O distance (*D*), typically 3–4 Å, and the C-H...O angle (*θ*). A radial scatter plot of *D* (Å) as a function of the angle *θ* (°) for the aromatic methyl groups of all four compounds is shown in Fig. 9.

Included in Fig. 9 are the very strong intramolecular C-H...O bonds for DMAT (rhombs), DMAQ (triangles) and TMAT (circles) with *D* = 2.6–2.7 Å. And *θ* ≈ 90°, which presumably lead to their extremely efficient

hydrogen atom tunneling. Notably, the intramolecular C–H···O bond in DMDBS, which is known not to undergo hydrogen atom quantum mechanical tunneling, has a $D = 3.0 \text{ \AA}$ value. When intermolecular contacts are considered, DMAQ and DMAT possess 5 and 4 intermolecular C–H···O bonds with D ranging from 3.55 to 3.75 \AA . In contrast, the closest intermolecular C–H···O bond in DMDBS and TMAT occur at 3.9–4.0 \AA . Since it has been suggested that C–H···O hydrogen bond is primarily electrostatic and decreases in strength occur as a function of the inverse of the bond distance [16], D^{-1} , the closer and more numerous C–H···O bonds in DMAQ and DMAT may account for the slower methyl rotation in these two molecules, as observed by the ^2H NMR.

4. Discussion

All compounds studied here have methyl groups with $k_{\text{rot}} \geq 10^8 \text{ s}^{-1}$ at ambient temperature. Methyl rotation in DMDBS and TMAT remains in the fast exchange limit ($k_{\text{rot}} > 10^7 \text{ s}^{-1}$), even at the lowest temperatures analyzed. Only DMAT and DMAQ have methyl groups

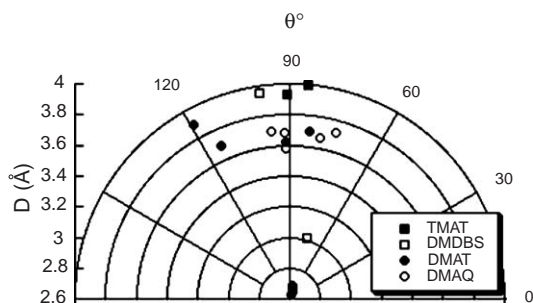


Fig. 9. Scatter plot of non-bonded C···O distances (D \AA) and C–H···O angles (θ°).

Table 2

Intramolecular parameters from XRD structures of the *ortho*-methylidibenzocycloalkanones studied in this work [sum of van der Waals radii]

| Ketone | <i>o</i> Me···O (\AA) | D (Me···CO) (deg) | <i>m</i> Me–X ₁ (\AA) | <i>m</i> Me···X ₂ (\AA) |
|--------|----------------------------------|---------------------|---|---|
| DMAT | 2.632 [3.2] | 1.673 0.2 | 2.830 ^a [2.9] | 2.829 ^a [2.9] |
| DMAQ | 2.686 [3.2] | 1.803 2.438 | 2.688 ^b [3.2] | — |
| DMDBS | 3.139 [3.2] | 56 | 2.549 ^c [2.9] | 3.823 ^c [2.9] |
| TMAT | 2.659 2.702 [3.2] | 12.8 14.8 | 3.234 ^d 3.167 ^e [3.4] | 3.854 ^d 3.182 ^e [3.2] |

^aDistance to the methylene hydrogens at C10.

^bDistance to the carbonyl oxygen.

^cDistance to the methylene at C11.

^{d,e}Distances to the methyl carbons at C10.

that approach the intermediate exchange regime with $k_{\text{rot}} \approx 10^6 \text{ s}^{-1}$ below 120 K. Given the limited kinetic data, it is not possible to draw reliable activation parameters for methyl rotation in the compounds studied. However, assuming a pre-exponential factor of ca. 10^{13} s^{-1} one can estimate approximate upper limits of ca. $E_a < 1.4$ and $E_a < 1.8 \text{ kcal/mol}$ for the fast and slow methyl groups of DMAT and DMAQ, and an upper limit of $E_a < 1.2 \text{ kcal/mol}$ for DMDBS and TMAT [7e]. Although aromatic methyl rotors are known to fall in this range (1–3 kcal/mol) [17], the effect of steric hindrance is somewhat counter intuitive. Our initial expectations were based on molecular models and the assumption that steric hindrance would increase the rotational barrier. Several structural parameters that can be used as indicators of steric hindrance are included in Table 2. Although the distance between methyl hydrogens and neighboring atoms would be the best indicator, hydrogen positions in the crystal structures are not accurate due to their low diffraction power and the position of rotating methyl hydrogens is particularly uncertain. However, a measure of intramolecular steric congestion encountered by the *ortho*-methyl groups may be given by the distance between the methyl carbon and the carbonyl oxygen, and by the torsion angle between the C–Me and C=O bond vectors of these two groups. An analogous indicator in the case of the *meta*-methyl groups at C4 is given by the distance between the methyl carbon and the neighboring hydrogen atoms in DMAT and DMDBS, or the methyl groups at the quaternary C10 carbon in TMAT.

Based on structural parameters from XRD data, we expected the methyl dynamics of DMAT and DMAQ to be quite similar. In fact, these were the two compounds with the higher rotational barriers which could be slowed down by ca. 120 K. The two slightly difference rotation rates in DMAT are consistent with the different local environment of the two methyl groups in the

structure. However, the distinction between two methyl groups in the DMAQ was unexpected based on the symmetry of the molecular structure and highlights the importance of the environment. Based on its molecular structure, methyl rotation in DMDBS was expected to be the fastest of the set. The methyl carbon to carbonyl oxygen distance is the longest of the four compounds and closest to the sum of the van der Waals radii. The *meta*-methyl group has a short contact with one of the two neighboring methylene hydrogens but is has a relatively long distance to the second one. The results obtained with TMAT were the most unanticipated. Based on its molecular structure, we expected its *ortho*-methyl group to be as hindered as that in DMAT and the *meta*-methyl group to be significantly more hindered. Although the two molecules in the unit cell have similar methyl carbon to carbonyl oxygen distances as that in DMAT, its rotational dynamics are significantly faster. Notably, the *meta*-methyl group also remains in the fast exchange limit despite the large steric congestion caused by the two methyl groups at C10.

5. Conclusions

The apparent steric congestion resulting from the close proximity of carbonyl and methyl groups is not manifested in terms of unusually high rotational barriers for the latter. In fact, methyl rotation in the solid state is remarkably fast and cannot be slowed down significantly at 115K. Activation barriers should be much greater than the average thermal energy available at 20 K (0.04 kcal/mol), strongly suggesting that methyl rotation is indeed slower than the hydrogen tunneling reactions that motivated this investigation.

Acknowledgments

We acknowledge a Professional Development Grant (#1311-11) from Mount St. Mary's College (DC), support from Drs. J. Strouse, R. Taylor and S. Khan. Support by NSF Grants CHE-0242270 and DMR-0307028 (MGG) is also acknowledged.

References

- [1] (a) M.A. Garcia-Garibay, A. Gamarnik, R. Bise, W.S. Jenks, *J. Am. Chem. Soc.* 117 (1995) 10264–10275;
(b) B.A. Johnson, M.A. Garcia-Garibay, *The Spectrum* 11 (1998) 1–7.
- [2] (a) B. Johnson, A. Gamarnik, M.A. Garcia-Garibay, *J. Phys. Chem.* 100 (1996) 4697–4700;
(b) B.A. Johnson, M.A. Garcia-Garibay, *J. Am. Chem. Soc.* 121 (1999) 8114–8115;
(c) B.A. Johnson, Y. Hu, K.N. Houk, M.A. Garcia-Garibay, *J. Am. Chem. Soc.* 123 (2001) 6941–6942;
(d) B.A. Johnson, M.H. Kleinman, N.J. Turro, M.A. Garcia-Garibay, *J. Org. Chem.* 67 (2002) 6944–6953.
- [3] R. Casadesus, M. Moreno, J.M. Lluch, *J. Phys. Chem. A* 108 (2004) 4536.
- [4] G.L. Hoatson, R.L. Vold, *NMR Basic Princ. Prog.* 32 (1994) 1–67.
- [5] L.W. Jelinsky, in: R.A. Komoroski (Ed.), *High-Resolution NMR Spectroscopy of Synthetic Polymers in Bulk*, VCH Publishers Inc., New York, 1986, pp. 335–364.
- [6] L.S. Batchelder, C.H. Niu, D.A. Torchia, *J. Am. Chem. Soc.* 105 (1983) 2228–2231.
- [7] (a) D.M. Rice, R.J. Wilteborg, R.G. Griffin, E. Meirovitch, E.R. Stimson, Y.C. Meinwald, J.H. Freed, H.A. Scheraga, *J. Am. Chem. Soc.* 103 (1981) 7707–7710;
(b) R.A. Kinsey, A. Kintanar, M. Tsai, R.L. Smith, N. Janes, E. Oldfield, *J. Biol. Chem.* 256 (1981) 4146–4149;
(c) K. Beshah, E.T. Olejniczak, R.G. Griffin, *J. Chem. Phys.* 86 (1987) 4730–4736;
(d) K. Beshah, R.G. Griffin, *J. Magn. Reson.* 84 (1989) 268–274;
(e) V. Copie, A.E. McDermott, K. Beshah, J.C. Williams, M. Spijker-Assink, R. Gebhard, J. Lugdenburg, J. Herzfeld, R. Griffin, *J. Biochem.* 33 (1994) 3280–3286.
- [8] (a) H.W. Spiess, *Colloid Polym. Sci.* 261 (1983) 193;
(b) H.W. spiess, *J. Mol. Struct.* 111 (1983) 119;
(c) H.W. spiess, *Adv. Polym. Sci.* 66 (1985) 23;
(d) J.J. Dumais, A.L. Cholli, L.W. Jelinsky, J.L. Hedrich, J.E. Mcgarth, *Macromolecules* (1986) 18.
- [9] P. Meier, E. Ohmes, G. Kothe, A. Blume, J. Weidner, H.-J. Eibl, *J. Phys. Chem.* 87 (1983) 4904.
- [10] (a) S. Nishikory, C.I. Ratcliffe, J.A. Ripmeester, *J. Phys. Chem.* 95 (1991) 1589–1596;
(b) S. Nishikory, C.I. Ratcliffe, J.A. Ripmeester, *Can. J. Chem.* 71 (1993) 1810–1815;
(c) S. Nishikory, T. Kitazawa, C. Kim, T. Iwamoto, *J. Phys. Chem.* 104 (2000) 2591–2598.
- [11] Z. Dominguez, H. Dang, M.J. Strouse, M-A. Garcia-Garibay, *J. Am. Chem. Soc.* 105 (2002) 2398–2399.
- [12] (a) D.Y. Curtin, R.C. Tuites, D.H. Dybuij, *J. Org. Chem.* 25 (1960) 155;
(b) S. Nishikory, T. Kitazawa, C. Kim, T. Iwamoto, *J. Phys. Chem.* 104 (2000) 2591–2598.
- [13] J.N. Chatterjea, H. Mukherjee, The synthesis of DMBS was first reported in, *J. Ind. Chem. Soc.* 37 (1960) 443–450.
- [14] R.J. Wilteborg, E.T. Olejniczak, R.G. Griffin, *J. Chem. Phys.* 86 (1987) 5411–5420.
- [15] E.L. Eliel, S.H. Wilen, *Stereochemistry of Organic Compounds*, Wiley, New York, 1994.
- [16] (a) G.R. Desiraju, *Acc. Chem. Res.* 24 (1991) 290–296;
(b) R. Taylor, O. Kennard, *J. Am. Chem. Soc.* 104 (1982) 5063–5070.
- [17] (a) P.A. Beckmann, C. Dybowski, E.J. Gaffney, C.W. Mallory, F.B. Mallory, *J. Phys. Chem. A* 105 (2001) 7350–7355;
(b) P.A. Beckmann, C.A. Buser, K. Gullifer, F.B. Mallory, C.W. Mallory, G.M. Rossi, A.L. Rheingold, *J. Chem. Phys.* 118 (2003) 11129–11138.